Statistics and Applications {ISSN 2454-7395 (online)}
Volume 23, No. 2, 2025 (New Series), pp 119–137
http://www.ssca.org.in/journal

Wrapped Generalized Lindley Distribution with Applications to Directional Data

Imliyangba and Bhanita Das
Department of Statistics, North Eastern Hill University, Shillong-793022

Received: 27 May 2024; Revised: 06 October 2024; Accepted: 08 October 2024

Abstract

The standard statistical techniques are fit to the linear data, where data are simply presented on a straight line. However, in many diverse scientific fields, the measurements are referred to as directions. Since a direction has no magnitude, these directions can be conveniently represented as points on the circumference of a unit circle centered at the origin or as a unit vector in the plane. In this article, the wrapped generalized Lindley distribution, a new class of circular distribution based on the wrapping method was introduced. Furthermore, the trigonometric moments and fundamental properties of the new circular distribution were studied. The method of maximum likelihood estimation was used to estimate the values of the parameter. A simulation study was performed to illustrate the proposed distribution in modeling directional data. The flexibility of the proposed model was shown by analyzing real-life data and its performance was compared with other families of circular Lindley distributions.

Key words: Wrapped distributions; Lindley distribution; Trigonometric moments; Maximum likelihood estimation; Angular data analysis.

1. Introduction

In many scientific experiments such as geological (Rao and Sengupta, 1972), medical Jammalamadaka *et al.* (1986), meteorological (Fisher, 1995), biological sciences (Jammalamadaka and Sengupta, 2001), *etc.*, the data have been observed exhibiting periodic or cyclic behaviors. The standard statistical techniques are not appropriate to handle these situations where the data are circular (directional). Therefore, to deal with such data and to perform statistical analysis, many circular distributions have been introduced from the existing linear distributions by adopting a variety of techniques namely wrapping, inverse stereographic projections, rising sun function, *etc.*

Perhaps the most popular technique to analyze circular data is the idea of wrapping a linear distribution around the unit circle which gives rise to a multitude of wrapped circular distributions. PL (1939) first introduced the wrapped distribution, and since then several wrapped versions of common probability distributions on the real line have been studied

Corresponding Author: Bhanita Das
Email: bhanitadas83@gmail.com

in the literature, including wrapped normal (Mardia and Jupp, 2000), wrapped Cauchy (Jammalamadaka and Sengupta, 2001), and wrapped stable distributions (Gatto and Jammalamadaka, 2003).

Further, Jammalamadaka and Kozubowski (2004) discussed the wrapped exponential and wrapped Laplace distributions and presented the explicit forms for their densities and distribution functions, as well as their trigonometric moments and related parameters. Pewsey *et al.* (2007) considered the three-parameter family of symmetric unimodal distributions obtained by wrapping the location-scale extension of Student's t distribution onto the unit circle. Coelho (2007) obtained an expression for the probability density function of the wrapped gamma distribution and illustrated both integer and non-integer shape parameters, as a mixture of truncated gamma distributions. Pewsey (2008) also considered the use of the wrapped stable family as a model for unimodal circular data. Sarma *et al.* (2011) presented certain population characteristics of the wrapped Lognormal and the wrapped Weibull distributions. In another work, Roy and Adnan (2012), Jacob and Jayakumar (2013), and Adnan and Roy (2014) explored wrapped generalized Gompertz distribution, wrapped geometric distribution and wrapped variance gamma distribution, respectively, and discussed their applications to circular data. Joshi and Jose (2018) introduced a new circular distribution called the wrapped Lindley distribution and derived expressions for characteristic function, trigonometric moments, coefficients of skewness, and kurtosis with an application to real-life datasets.

In the recent past, Shanker *et al.* (2013) introduced the generalized Lindley (GL) distribution as a special case of the one-parameter Lindley distribution (Lindley, 1958). Over the years, the GL distribution has emerged as a new lifetime model that is more applicable than the Lindley distribution. Several researchers have introduced many modified versions of the GL distribution and shown its applicability in diverse data environments through parameterization which is linear in nature. However, most works on GL distribution are limited to random variables with an infinite set of possible values. Therefore, the authors were motivated to apply the concept of circular statistics to the GL distribution by reducing its modulo 2π with the help of the wrapping technique. The main objective of this article was to propose a new generalized Lindley distribution by wrapping the density along a unit circle, called the wrapped generalized Lindley (WGL) distribution. This article also aimed to study the properties of the proposed distribution, and explore its utility as a circular model.

The rest of the paper is organized as follows. Section 2 describes the wrapping technique and introduces a new WGL distribution. Section 3 graphically illustrates the behavior of the newly developed distribution. The derivations of the characteristic function and the trigonometric moments as well as the associated parameters are discussed in Section 4 and Section 5, respectively. Section 6 examines the estimation of the parameters using the maximum likelihood method. A simulation study is discussed in Section 7, to show the consistency of the estimator. In Section 8, we fit the proposed distribution to five circular datasets and compare its performance with other competing wrapped distributions. Finally, conclusions are made in Section 9.

2. Definition and derivation

2.1. Wrapped distribution

Any linear random variable (r.v.) X on the real line may be transformed to a circular random variable by reducing its modulo 2π *i.e.*, we define

$$\theta = X(mod\ 2\pi)$$

This operation corresponds to taking the real line and wrapping it around the circle of unit radius, accumulating probability over all the overlapping points $x = \theta, \theta \pm 2\pi, \theta \pm 4\pi, \ldots$. This is a many-to-one mapping so that if $g(\theta)$ represents the circular density and *f(x)* the density of the real-valued r.v., we have

$$g(\theta) = \sum_{m=-\infty}^{\infty} f(\theta + 2\pi m), 0 \leq \theta < 2\pi \tag{1}$$

By this technique, both discrete and continuous wrapped distributions may be constructed.

2.2. Wrapped generalized Lindley distribution

The probability density function (*pdf*) of the generalized Lindley distribution given by Shanker *et al.* (2013) is,

$$f(x;\lambda,\alpha) = \frac{\lambda^2}{\alpha(\lambda+\alpha^2)}(1+\alpha x)e^{-\frac{\lambda}{\alpha}x};\ x > 0, \lambda > 0, \alpha > 0 \tag{2}$$

Using equations (1) and (2), the *pdf* of the WGL distribution is derived as given below,

$$\begin{aligned} g(\theta) &= \sum_{m=0}^{\infty} f(\theta + 2\pi m) \\ &= \sum_{m=0}^{\infty} \frac{\lambda^2}{\alpha(\lambda+\alpha^2)} \left\{1 + \alpha(\theta + 2\pi m)\right\} e^{-\frac{\lambda}{\alpha}(\theta+2\pi m)} \\ &= \frac{\lambda^2}{\alpha(\lambda+\alpha^2)} e^{-\frac{\lambda}{\alpha}\theta} \left\{ \frac{(1+\alpha\theta)}{1-e^{-2\pi\frac{\lambda}{\alpha}}} + \frac{2\pi\alpha e^{-2\pi\frac{\lambda}{\alpha}}}{(1-e^{-2\pi\frac{\lambda}{\alpha}})^2} \right\} \end{aligned} \tag{3}$$

The cummulative distribution function (*cdf*) of the wrapped distribution is given by

$$G(\theta) = \sum_{m=0}^{\infty} F(\theta + 2\pi m) - F(2\pi m)$$

Therefore, the *cdf* of the WGL distribution is obtained as

$$\begin{aligned}
G(\theta) &= \sum_{m=0}^{\infty}\left[\left\{1-\frac{\alpha(\lambda+\alpha^2)+\lambda\alpha^2(\theta+2\pi m)}{\alpha(\lambda+\alpha^2)}e^{-\frac{\lambda}{\alpha}(\theta+2\pi m)}\right\}-\right.\\
&\qquad\left.\left\{1-\frac{\alpha(\lambda+\alpha^2)+\lambda\alpha^2 2\pi m}{\alpha(\lambda+\alpha^2)}e^{-\frac{\lambda}{\alpha}(2\pi m)}\right\}\right]\\
&= \sum_{m=0}^{\infty}\frac{1}{\alpha(\lambda+\alpha^2)}\left[\alpha(\lambda+\alpha^2)e^{-\frac{\lambda}{\alpha}(2\pi m)}+\lambda\alpha^2 2\pi m e^{-\frac{\lambda}{\alpha}(2\pi m)}-\right.\\
&\qquad\left.\left\{\alpha(\lambda+\alpha^2)+\lambda\alpha^2(\theta+2\pi m)e^{-\frac{\lambda}{\alpha}(\theta+2\pi m)}\right\}\right]\\
&= \frac{1}{\alpha(\lambda+\alpha^2)}\left[\alpha(\lambda+\alpha^2)\sum_{m=0}^{\infty}e^{-\frac{\lambda}{\alpha}(2\pi m)}+\lambda\alpha^2 2\pi\sum_{m=0}^{\infty}m e^{-\frac{\lambda}{\alpha}(2\pi m)}-\right.\\
&\qquad\left.\left\{\alpha(\lambda+\alpha^2)e^{-\frac{\lambda}{\alpha}\theta}\sum_{m=0}^{\infty}e^{-\frac{\lambda}{\alpha}(2\pi m)}+\lambda\alpha^2 e^{-\frac{\lambda}{\alpha}\theta}\sum_{m=0}^{\infty}(\theta+2\pi m)e^{-\frac{\lambda}{\alpha}(2\pi m)}\right\}\right]\\
&= \left(\frac{1}{1-e^{-2\pi\frac{\lambda}{\alpha}}}\right)\left\{1-e^{-\frac{\lambda}{\alpha}\theta}-\frac{(\lambda\alpha^2\theta e^{-\frac{\lambda}{\alpha}})}{\alpha(\lambda+\alpha^2)}\right\}+\frac{2\pi\lambda\alpha^2}{\alpha(\lambda+\alpha^2)}\left(1-e^{-\frac{\lambda}{\alpha}\theta}\right)\frac{e^{-2\pi\frac{\lambda}{\alpha}}}{(1-e^{-2\pi\frac{\lambda}{\alpha}})^2} \quad (4)
\end{aligned}$$

3. Graphical representations of WGL distribution

The following figures provide a linear representation of WGL distribution for some special cases.

3.1. Linear representation of WGL distribution

Case 1: When $\lambda < \alpha$, **Case 2**: When $\lambda > \alpha$, and **Case 3**: When $\lambda = \alpha$.

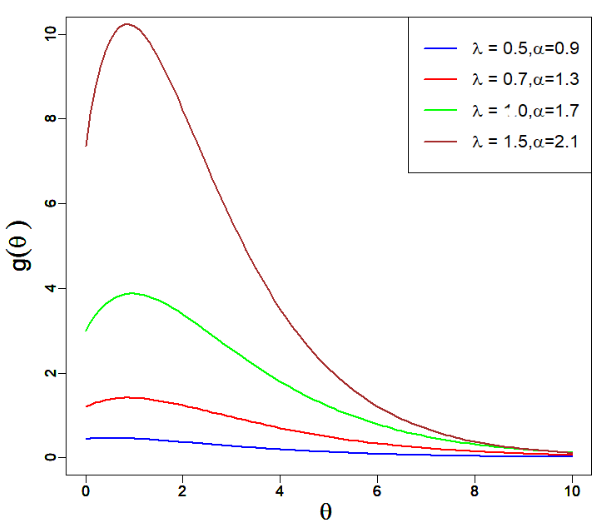

Figure 1: Graphical representation of WGL distribution when $\lambda < \alpha$

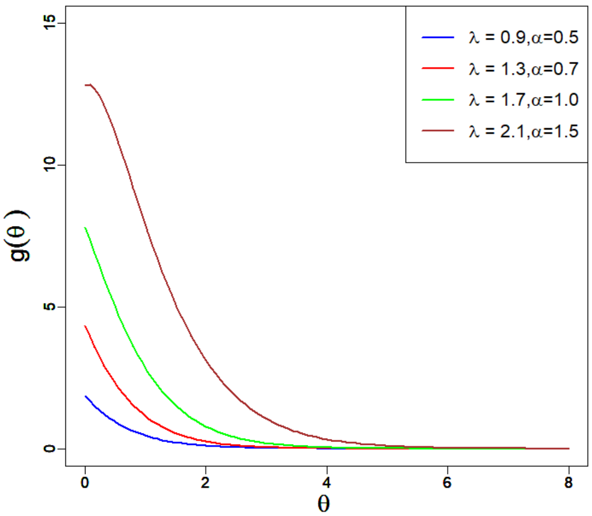

Figure 2: Graphical representation of WGL distribution when $\lambda > \alpha$

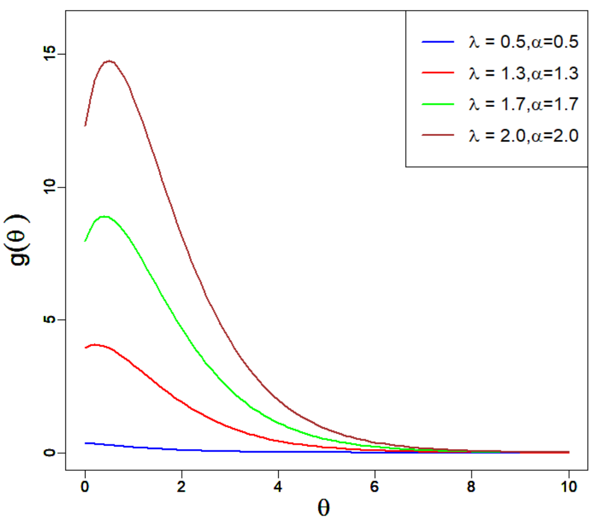

Figure 3: Graphical representation of WGL distribution when $\lambda = \alpha$

From the three graphs of WGL distribution in Figure 1, Figure 2 and Figure 3 we can make the following observations:

- Figure 1, Figure 2 and Figure 3 show some of the possible shapes of the *pdf* of WGL distribution for different values of the parameters λ and α.
- Figure 1 represents the *pdf* of WGL distribution when $\lambda < \alpha$. As the values of both the parameter increase, we get a positively high kurtosis with low skewness.
- When $\lambda > \alpha$, the curve of WGL distribution shows an exponentially decreasing behav-

ior with positively low skewness. Figure 2 also justifies that the proposed distribution inherits the properties of Exponential distribution where GL distribution can be shown as a mixture of Exponential $(\frac{\lambda}{\alpha})$ and Gamma distribution $(2, \frac{\lambda}{\alpha})$(Shanker *et al.*, 2013).

- Figure 3 represents the shape of WGL distribution when $\lambda = \alpha$ which shows a positively high kurtosis and positively low skewness with more peakedness and lesser tail as compared to Figure 1.

The above observations (Figure 1, Figure 2 and Figure 3) justify the graphical representation of the proposed distribution. Moreover, we can conclude that the proposed distribution can be used to model the datasets with decreasing and increasing-decreasing behaviors.

3.2. Circular representation of WGL distribution

Figure 4 and Figure 5 display the circular representation of WGL distribution with different values of the parameter α, keeping $\lambda = 1.5$ in Figure 4 and with the changing values of the parameter λ, keeping α constant in Figure 5.

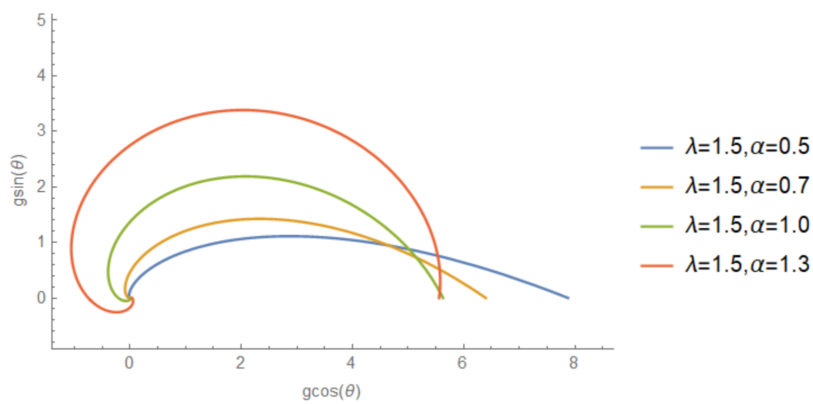

Figure 4: Circular representation of WGL distribution when λ is constant

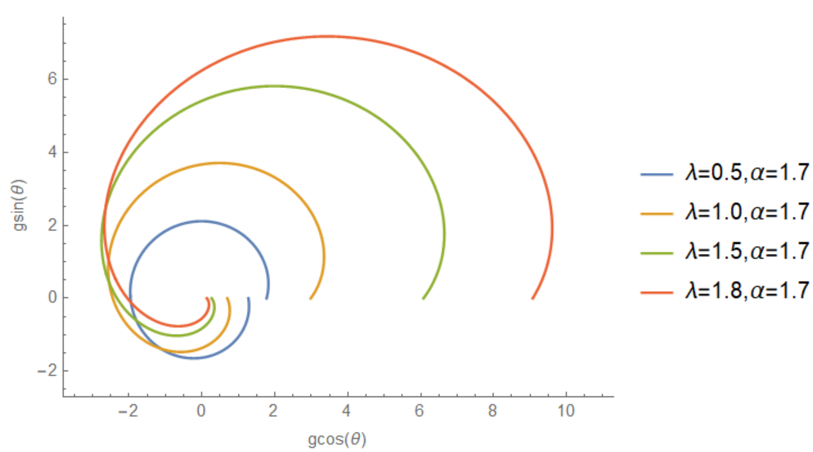

Figure 5: Circular representation of WGL distribution when α is constant

4. Characteristic function

According to Jammalamadaka and Sengupta (2001), the trigonometric moments of order p for a wrapped circular distribution corresponds to the value of the characteristic function of the unwrapped r.v. X, say $\varphi_x(t)$ at the integer value, *i.e.*,

$$\varphi(p) = \varphi_x(t)$$

The characteristic function of GL distribution is given by,

$$\begin{aligned}
\varphi_x(t) &= E(e^{itx}) \\
&= \frac{\lambda^2}{\alpha(\lambda+\alpha^2)} \int_0^\infty (1+\alpha x) e^{-\frac{\lambda}{\alpha}x} e^{itx} dx \\
&= \frac{\lambda^2}{\alpha(\lambda+\alpha^2)} \left\{ \frac{1}{\frac{\lambda}{\alpha} - it} - \frac{\alpha}{(\frac{\lambda}{\alpha} - it)^2} \right\} \\
&= \frac{\lambda^2}{\alpha(\lambda+\alpha^2)} \left[\frac{\frac{\lambda}{\alpha} - \alpha - it}{(\frac{\lambda}{\alpha} - it)^2} \right]
\end{aligned}$$

Therefore, the characteristic function of WGL distribution is given by,

$$\varphi(p) = \frac{\lambda^2}{\alpha(\lambda+\alpha^2)} \left[\frac{\frac{\lambda}{\alpha} - \alpha - ip}{(\frac{\lambda}{\alpha} - ip)^2} \right] \tag{5}$$

where $i = (-1)^{\frac{1}{2}}$ and $p = \pm 1, \pm 2, ...$

From Roy and Adnan (2012), $\forall\ a, b, r \in R^+$,

$$(a - ib)^{-r} = (a^2 + b^2)^{-\frac{r}{2}}\ exp\left\{ir\ arctan\left(\frac{b}{a}\right)\right\}$$

The following expressions are obtained

$$\left(\frac{\lambda}{\alpha} - ip\right)^{-2} = \left\{\left(\frac{\lambda}{\alpha}\right)^2 + p^2\right\}^{-1}\ exp\left\{2i\ arctan\ p\left(\frac{\alpha}{\lambda}\right)\right\}$$

$$\left(\frac{\lambda}{\alpha} - \alpha - ip\right)^{1} = \left\{\left(\frac{\lambda}{\alpha} - \alpha\right)^2 + p^2\right\}^{-\frac{1}{2}}\ exp\left\{i\ arctan\left(\frac{p}{\frac{\lambda}{\alpha} - \alpha}\right)\right\}$$

About the above expressions, equation (5) may be finally written as,

$$\varphi(p) = \frac{\lambda^2\left\{\left(\frac{\lambda}{\alpha} - \alpha\right)^2 + p^2\right\}^{-\frac{1}{2}}}{\alpha(\lambda+\alpha^2)\left\{\left(\frac{\lambda}{\alpha}\right)^2 + p^2\right\}^{-1}}\ exp\left\{2i\ arctan\ p\left(\frac{\alpha}{\lambda}\right) - i\ arctan\left(\frac{p}{\frac{\lambda}{\alpha} - \alpha}\right)\right\} \tag{6}$$

and so,

$$\varphi(p) = \rho_p e^{i\mu_p} \tag{7}$$

Comparing equation (7) to (6), we get

$$\rho_p = \frac{\lambda^2 \left\{ \left(\frac{\lambda}{\alpha} - \alpha \right)^2 + p^2 \right\}^{-\frac{1}{2}}}{\alpha(\lambda + \alpha^2) \left\{ \left(\frac{\lambda}{\alpha} \right)^2 + p^2 \right\}^{-1}}$$

$$\begin{aligned} \mu_p &= 2\ arctan\ p \left(\frac{\alpha}{\lambda} \right) -\ arctan \left(\frac{p}{\frac{\lambda}{\alpha} - \alpha} \right) \\ &= arctan\ p \left\{ 2 \left(\frac{\alpha}{\lambda} \right) - \left(\frac{\alpha}{\lambda - \alpha^2} \right) \right\} \end{aligned}$$

5. Trigonometric moments and related parameters

According to the definition of the trigonometric moment,

$$\Phi_p = \alpha_p + i\beta_p; \quad p = \pm 1, \pm 2, ...$$

Therefore, the non-central trigonometric moments of the respective distribution are defined as,

$$\alpha_p = \rho_p\ cos\ \mu_p \ \text{ and } \ \beta_p = \rho_p\ sin\ \mu_p$$

So, we have

$$\alpha_p = \frac{\lambda^2 \left\{ \left(\frac{\lambda}{\alpha} - \alpha \right)^2 + p^2 \right\}^{-\frac{1}{2}}}{\alpha(\lambda + \alpha^2) \left\{ \left(\frac{\lambda}{\alpha} \right)^2 + p^2 \right\}^{-1}}\ cos \left\{ 2\ arctan\ p \left(\frac{\alpha}{\lambda} \right) -\ arctan \left(\frac{p}{\frac{\lambda}{\alpha} - \alpha} \right) \right\}$$

$$\beta_p = \frac{\lambda^2 \left\{ \left(\frac{\lambda}{\alpha} - \alpha \right)^2 + p^2 \right\}^{-\frac{1}{2}}}{\alpha(\lambda + \alpha^2) \left\{ \left(\frac{\lambda}{\alpha} \right)^2 + p^2 \right\}^{-1}}\ sin \left\{ 2\ arctan\ p \left(\frac{\alpha}{\lambda} \right) -\ arctan \left(\frac{p}{\frac{\lambda}{\alpha} - \alpha} \right) \right\}$$

Now, the central trigonometric moments are

$$\bar{\alpha}_p = \rho_p\ cos(\mu_p - p\mu_1) \ \text{ and } \ \bar{\beta}_p = \rho_p\ sin(\mu_p - p\mu_1)$$

Thus, the central trigonometric moments of WGL distribution will be

$$\begin{aligned} \bar{\alpha}_p = & \frac{\lambda^2 \left\{ \left(\frac{\lambda}{\alpha} - \alpha \right)^2 + p^2 \right\}^{-\frac{1}{2}}}{\alpha(\lambda + \alpha^2) \left\{ \left(\frac{\lambda}{\alpha} \right)^2 + p^2 \right\}^{-1}}\ cos \left[2\ arctan\ p \left(\frac{\alpha}{\lambda} \right) -\ arctan \left(\frac{p}{\frac{\lambda}{\alpha} - \alpha} \right) - \right. \\ & \left. \left\{ 2\ arctan\ \left(\frac{\alpha}{\lambda} \right) -\ arctan \left(\frac{1}{\frac{\lambda}{\alpha} - \alpha} \right) \right\} \right] \end{aligned}$$

$$\bar{\beta}_p = \frac{\lambda^2\left\{\left(\frac{\lambda}{\alpha}-\alpha\right)^2+p^2\right\}^{-\frac{1}{2}}}{\alpha(\lambda+\alpha^2)\left\{\left(\frac{\lambda}{\alpha}\right)^2+p^2\right\}^{-1}}\ sin\left[2\ arctan\ p\left(\frac{\alpha}{\lambda}\right)-\ arctan\left(\frac{p}{\frac{\lambda}{\alpha}-\alpha}\right)-\right.$$
$$\left.\left\{2\ arctan\ \left(\frac{\alpha}{\lambda}\right)-\ arctan\left(\frac{1}{\frac{\lambda}{\alpha}-\alpha}\right)\right\}\right]$$

Since we have

$$\mu_p = arctan\ p\left\{2\left(\frac{\alpha}{\lambda}\right)-\left(\frac{\alpha}{\lambda-\alpha^2}\right)\right\}$$

For $p = 1$

$$\mu_1 = arctan\ \left\{2\left(\frac{\alpha}{\lambda}\right)-\left(\frac{\alpha}{\lambda-\alpha^2}\right)\right\}$$

Moreover, the resultant length is $\rho = \rho_1$

$$\rho = \frac{\lambda^2\left\{\left(\frac{\lambda}{\alpha}-\alpha\right)^2+1\right\}^{-\frac{1}{2}}}{\alpha(\lambda+\alpha^2)\left\{\left(\frac{\lambda}{\alpha}\right)^2+1\right\}^{-1}}$$

The mean direction is,

$$\mu = \mu_1$$
$$\mu_1 = arctan\ \left\{2\left(\frac{\alpha}{\lambda}\right)-\left(\frac{\alpha}{\lambda-\alpha^2}\right)\right\}$$

The mean direction gives information about the mean of the distribution as an analogy of the mean in the linear distributions and the resultant length is a measure of dispersion around the mean which corresponds to the usual standard deviation or variance in linear distributions. The circular variance is,

$$V_0 = 1-\rho$$

$$V_0 = 1-\frac{\lambda^2\left\{\left(\frac{\lambda}{\alpha}-\alpha\right)^2+1\right\}^{-\frac{1}{2}}}{\alpha(\lambda+\alpha^2)\left\{\left(\frac{\lambda}{\alpha}\right)^2+1\right\}^{-1}}$$

The circular standard deviation is,

$$\begin{aligned}\sigma_0 &= \sqrt{-2\log(1-V_0)}\\ &= \sqrt{-2\log\left(1-1+\frac{\lambda^2\left\{\left(\frac{\lambda}{\alpha}-\alpha\right)^2+1\right\}^{-\frac{1}{2}}}{\alpha(\lambda+\alpha^2)\left\{\left(\frac{\lambda}{\alpha}\right)^2+1\right\}^{-1}}\right)}\\ &= \sqrt{-2\log\left(\frac{\lambda^2\left\{\left(\frac{\lambda}{\alpha}-\alpha\right)^2+1\right\}^{-\frac{1}{2}}}{\alpha(\lambda+\alpha^2)\left\{\left(\frac{\lambda}{\alpha}\right)^2+1\right\}^{-1}}\right)}\end{aligned}$$

The skewness $\xi_1^0 = \frac{\bar{\beta}_2}{V_0^{\frac{3}{2}}}$ is given by,

$$\xi_1^0 = \frac{\frac{\lambda^2\left\{\left(\frac{\lambda}{\alpha}-\alpha\right)^2+4\right\}^{-\frac{1}{2}}}{\alpha(\lambda+\alpha^2)\left\{\left(\frac{\lambda}{\alpha}\right)^2+4\right\}^{-1}} \; sin\left[arctan\ 2\ \left\{\left(\frac{\alpha}{\lambda}\right)-\left(\frac{\alpha}{\lambda-\alpha^2}\right)\right\}-2\ arctan\ \left\{\left(\frac{\alpha}{\lambda}\right)-\left(\frac{\alpha}{\lambda-\alpha^2}\right)\right\}\right]}{\left\{1-\frac{\lambda^2\left\{\left(\frac{\lambda}{\alpha}-\alpha\right)^2+1\right\}^{-\frac{1}{2}}}{\alpha(\lambda+\alpha^2)\left\{\left(\frac{\lambda}{\alpha}\right)^2+1\right\}^{-1}}\right\}^{\frac{3}{2}}}$$

And the kurtosis is given by

$$\xi_2^0 = \frac{\bar{\alpha}_2-(1-V_0)^4}{V_0^2}$$

where

$$\bar{\alpha}_2 = \frac{\lambda^2\left\{\left(\frac{\lambda}{\alpha}-\alpha\right)^2+4\right\}^{-\frac{1}{2}}}{\alpha(\lambda+\alpha^2)\left\{\left(\frac{\lambda}{\alpha}\right)^2+4\right\}^{-1}} \; cos\left[2\ arctan\ 2\left(\frac{\alpha}{\lambda}\right)-\ arctan\left(\frac{2}{\frac{\lambda}{\alpha}-\alpha}\right)-\right.$$
$$\left.\left\{2\ arctan\ \left(\frac{\alpha}{\lambda}\right)-\ arctan\left(\frac{1}{\frac{\lambda}{\alpha}-\alpha}\right)\right\}\right]$$

$$V_0 = 1-\frac{\lambda^2\left\{\left(\frac{\lambda}{\alpha}-\alpha\right)^2+1\right\}^{-\frac{1}{2}}}{\alpha(\lambda+\alpha^2)\left\{\left(\frac{\lambda}{\alpha}\right)^2+1\right\}^{-1}}$$

The values of the various descriptive measures for some particular values of α and λ are summarized in Table 1.

From Table 1, we can make the following remarks:

- The mean direction increases with the change in λ keeping α constant as well as with different values of α keeping λ as constant. However, the resultant length decreases with the change in α and λ.
- The mean direction approaches 1 as α increases.
- The circular variance increases with the increase in α and λ.

6. Maximum likelihood estimation

The method of maximum likelihood estimation is one of the most important techniques in statistics and econometrics for estimating the parameters. Let $\theta_1, \theta_2, \ldots, \theta_n$ be a random sample of size n from WGL distribution. Then, the likelihood function is given by,

$$L = \left\{\frac{\lambda^2}{\alpha(\lambda+\alpha^2)}\right\}^n e^{-\frac{\lambda}{\alpha}\sum_{i=1}^n \theta_i} \sum_{i=1}^n \left\{\frac{1+\alpha\theta_i}{1-e^{-\frac{\lambda}{\alpha}2\pi}}+\frac{2\alpha\pi e^{-\frac{\lambda}{\alpha}2\pi}}{(1-e^{-\frac{\lambda}{\alpha}2\pi})^2}\right\}$$

Table 1: Values of different characteristics of the WGL distribution for various values of α and λ

α		0.5	0.5	0.5	1	1.5	2.5
λ		0.5	3.5	4.5	0.5	0.5	0.5
Mean direction	μ	0.288349	2.975447	1.799375	0.506719	0.523067	0.718435
Resultant length	ρ	0.989381	0.466179	0.182925	0.982512	0.968803	0.966841
Trigonometric moments	α_1	0.948534	-0.459759	-0.041449	0.859051	0.839266	0.727874
	α_2	0.802768	0.028768	0.031769	0.489695	0.437383	0.100793
	β_1	0.281351	0.077097	0.178167	0.476824	0.483955	0.636382
	β_2	0.522730	0.096061	-0.022027	0.792252	0.761552	0.867437
Central trigonometric moments	$\bar{\alpha_1}$	0.989381	0.466179	0.182925	0.982512	0.968803	0.966841
	$\bar{\alpha_2}$	0.957958	-0.004141	-0.018784	0.931371	0.878212	0.873128
	$\bar{\beta_1}$	0	0	0	0	0	0
	$\bar{\beta_2}$	0.000469	0.100191	0.033788	0.003477	0.002926	0.015935
Circular variance	V_0	0.010618	0.533820	0.817074	0.035918	0.064185	0.068678
Skewness	ξ_1^0	0.029535	0.146971	0.036656	1.503285	0.063031	0.323080
Kurtosis	ξ_2^0	-0.000245	-0.236381	-0.594824	-0.000510	-0.00290	-0.000740

And the log-likelihood function is

$$LogL = 2n\ log\ log\ \lambda - n\ log\ log\ \left\{\alpha(\lambda+\alpha^2)\right\} - \frac{\lambda}{\alpha}\sum_{i=1}^{n}\theta_i + \sum_{i=1}^{n} log\left\{\frac{1+\alpha\theta_i}{1-e^{-\frac{\lambda}{\alpha}2\pi}} + \frac{2\alpha\pi e^{-\frac{\lambda}{\alpha}2\pi}}{(1-e^{-\frac{\lambda}{\alpha}2\pi})^2}\right\} \tag{8}$$

The MLE of the parameters is computed by solving the maximum likelihood equations

$$\frac{\partial}{\partial\lambda}logL = 0,\ \text{and}\ \frac{\partial}{\partial\alpha}logL = 0 \tag{9}$$

Since the maximum likelihood equations cannot be solved analytically, therefore, a numerical technique is to be employed to get a solution for λ and α. We use statistical packages in R to get the maximum likelihood estimator (MLE) of the unknown parameters which is explained through simulation study.

7. Simulation study

A simulation study was performed to obtain the estimates of unknown parameters *i.e.*, λ and α. Further, a random sample of different sizes (n = 25, 50, 100, 200, 400, 500, 600) was generated for different values of λ and α, and replicated the program N=1000 times to get the MLE of λ and α. Given below is the algorithm for generating data from WGL distribution.

Step 1: Generate a random variable, say u, from $U(0,1)$.

Step 2: Equating the *cdf* given in equation (4) to u and solving it *w.r.t* θ, we get the WGL circular random variable.

Step 3: Substituting the WGL circular random variable, generated in step 2, in equation (9) and maximizing this *w.r.t* θ by using the maxLik package in R, we get the MLE of λ and α.

Step 4: To calculate the average bias and mean square error (MSE) of $\hat{\lambda}$ and $\hat{\alpha}$, we use the following formulae. Let λ^* and α^* be the true values of parameters λ and α, respectively. Then, the bias and MSE of $\hat{\lambda}$ and $\hat{\alpha}$ from true values of parameter λ^* and α^* are defined as:

$$bias(\hat{\lambda}) = \frac{1}{N}\sum_{i=1}^{N}(\hat{\lambda} - \lambda^*), \qquad MSE(\hat{\lambda}) = \frac{1}{N}\sum_{i=1}^{N}(\hat{\lambda} - \lambda^*)^2$$

$$bias(\hat{\alpha}) = \frac{1}{N}\sum_{i=1}^{N}(\hat{\alpha} - \alpha^*), \qquad MSE(\hat{\alpha}) = \frac{1}{N}\sum_{i=1}^{N}(\hat{\alpha} - \alpha^*)^2$$

Where N is the number of replications.

For $\lambda = 4$ and $\alpha = 1.6$, the estimated values of λ and α, and average values of bias and MSE for $\hat{\lambda}$ and $\hat{\alpha}$, are obtained in Table 2.

Table 2: Estimated values of λ and α, and average values of bias and MSE for $\hat{\lambda}$ and $\hat{\alpha}$

n	$\hat{\lambda}$	$\hat{\alpha}$	$\hat{\lambda}$		$\hat{\alpha}$	
			Bias	MSE	Bias	MSE
25	4.9460	2.1640	0.037840	0.035797	0.022560	0.012724
50	4.8430	1.9960	0.016860	0.014213	0.007920	0.079680
100	4.7491	1.9829	0.007491	0.005612	0.003829	0.039319
200	4.6653	1.9340	0.003327	0.002213	0.001670	0.018702
400	4.5750	1.8663	0.001438	0.000827	0.000666	0.008708
500	4.3006	1.8241	0.000601	0.000181	0.000448	0.006655
600	4.0895	1.6868	0.000149	0.000013	0.000145	0.004742

From Table 2, it is observed that, as the sample size increases, the estimated values of the parameters approach very close to the true values of parameters used in the simulation. Moreover, we can also see that the bias and MSE values for the estimated parameters decrease and tend to zero as the sample size increases. This shows the adequacy of the estimation technique.

8. Applications to circular datasets

One of the most important ways to justify the newly proposed distribution is the applicability of the distribution in real life. Therefore, to show the flexibility of the WGL distribution, the wrapped Lindley (WL), wrapped two-parameter Lindley (WTPL), wrapped exponential (WE), and the wrapped generalized Lindley (WGL) distributions were fitted to five circular datasets given below. Various statistics like Log-likelihood, AIC, AICC, and BIC were calculated and the results are shown in Table 3, Table 4, Table 5, Table 6, and Table 7.

First dataset: The application of the proposed distribution is illustrated by fitting it to a real-life dataset. The dataset consists of orientations of 76 turtles after laying eggs (PL, 1939) which are given in direction (in degrees) clockwise from North.

8, 9, 13, 13, 14, 18, 22, 27, 30, 34, 38, 38, 40, 44, 45, 47, 48, 48, 48, 48, 50, 53, 56, 57, 58, 58, 61, 63, 64, 64, 64, 65, 65, 68, 70, 73, 78, 78, 78, 83, 83, 88, 88, 88, 90, 92, 92, 93, 95, 96, 98, 100, 103, 106, 113, 118, 138, 153, 153, 155, 204, 215, 223, 226, 237, 238, 243, 244, 250, 251, 257, 268, 285, 319, 343, 350.

The dataset is fitted to the proposed distribution and the plot is given in Figure 6. Comparing Figure 6 with that of the graph of WGL distribution in Figure 2, we can say that WGL distribution is appropriate to model the given dataset.

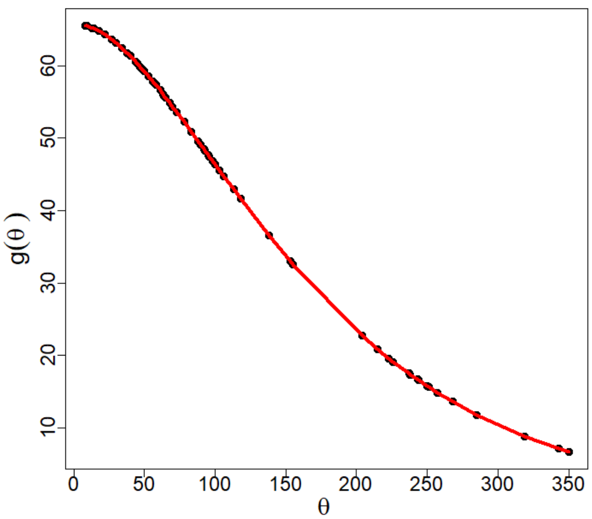

Figure 6: Graph of orientations of 76 turtles after laying eggs

Table 3: Summary of statistics for WL, WTPL, WE, and WGL distributions for the first dataset

Distribution	MLE	Log-likelihood	AIC	BIC	AICC
WL	$\lambda = 0.2163$	-62.223	-120.446	-115.759	-120.284
WTPL	$\theta = 1.151 \times 10^{-6}$ $\alpha = 0.6685$	-79.86	-155.72	-151.01	-155.56
WE	$\lambda = 1.213 \times 10^{-6}$	-83.044	-162.09	-157.4	-161.93
WGL	$\lambda = 0.0525$ $\alpha = 0.0464$	-87.355	-170.709	-165.996	-170.549

Second dataset: The second dataset includes pigeon homing experimental data (Pewsey, 2008). The experiment consists of 13 birds that were released singly in the Toggenburg valley and their vanishing angles (in degrees) were recorded. The dataset is given below:

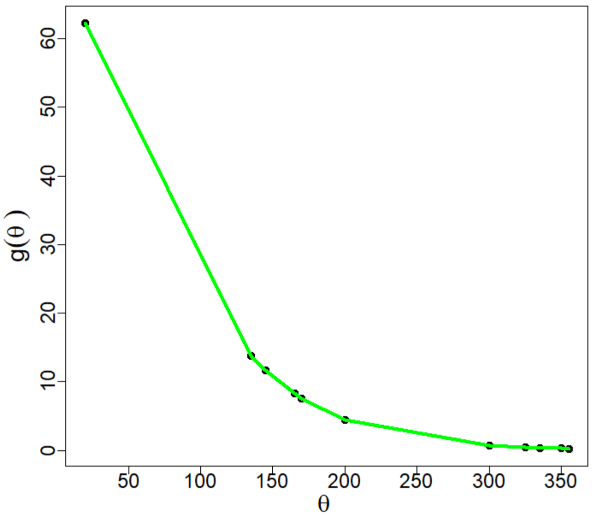

Figure 7: Graph of vanishing angles of 13 birds

20, 135, 145, l65, 170, 200, 300, 325, 335, 350, 350, 350, 355.

Figure 7 displays the graphical representation of pigeon homing experimental data which includes the vanishing angles of 13 birds. From the graph of vanishing angles of 13 birds, we get some similar shape behaviors with that of WGL distribution, given in Figure 1, Figure 2 and Figure 3. Therefore, the given dataset *i.e.*, vanishing angles of 13 birds, can be fitted with the proposed WGL distribution.

Table 4: Summary of statistics for WL, WTPL, WE, and WGL distributions for second dataset

Distribution	MLE	Log-likelihood	AIC	BIC	AICC
WL	$\lambda = 0.5178$	-0.953	2.094	3.372	3.185
WTPL	$\theta = 0.3112$ $\alpha = 1.429 \times 10^{-10}$	-4.251	-4.502	-3.086	-3.502
WE	$\lambda = 2.5750$	-2.546	-1.092	0.186	-0.001
WGL	$\lambda = 0.0890$ $\alpha = 0.0288$	-9.576	-15.152	-13.735	-14.152

Third dataset: The third dataset was taken from Fisher (1995). The dataset includes the orientations of the nest of 50b noisy scrub birds along the bank of a creek bed and the data (in degree) are as given below:

160, 145, 225, 230, 295, 295, 140, 140, 140, 205, 215, 135, 110, 240, 230, 250, 30, 215, 215, 135, 110, 240, 105, 125, 125, 130, 160, 105, 90, 130, 200, 240, 105, 125, 125, 125, 130, 160, 160, 250, 200, 200, 240, 240, 240, 250, 250, 250, 140, 140.

Figure 8 shows the graph of orientations of the nest of 50b noisy scrub birds. The following are some of the reasons for modeling and analyzing the datasets of the orientations

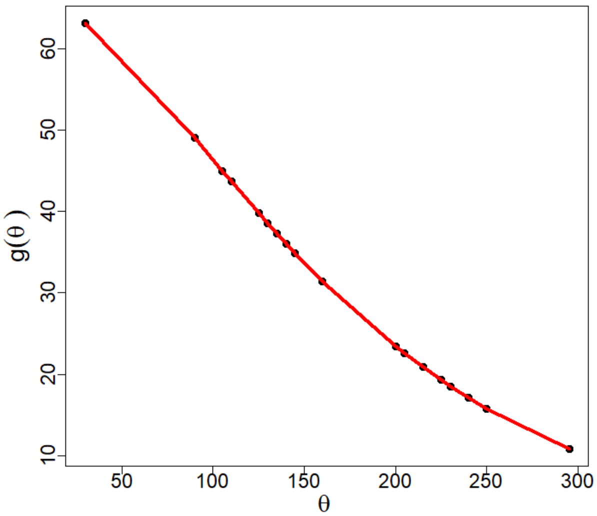

Figure 8: Graph of orientations of the nest of 50b noisy scrub birds

of the nest of 50b noisy scrub birds, directions of 22 sea stars 11 days after being displaced from their natural habitat, and the time series of 72 wind directions, with the WGL distribution. Firstly, Figure 8, Figure 9, and Figure 10 follow some of the characteristics and behaviors of the WGL distribution which can be compared with that of Figure 2. Secondly, all three datasets were measured in degrees that were circular in nature.

Table 5: Summary of statistics for WL, WTPL, WE, and WGL distributions for third dataset

Distribution	MLE	Log-likelihood	AIC	BIC	AICC
WL	$\lambda = 0.1034$	-59.128	-114.255	-110.392	-114.005
WTPL	$\theta = 0.05178$ $\alpha = 2.102 \times 10^{-10}$	-58.216	-112.431	-108.529	-112.186
WE	$\lambda = 2.305$	-50.891	-97.782	-93.918	-97.532
WGL	$\lambda = 0.0456$ $\alpha = 0.0419$	-65.973	-127.947	-124.044	-127.702

Fourth dataset: Further, to demonstrate the modeling potential of the WGL distribution, sea star movements were considered as reported by Upton (1985) and discussed later by Fisher (1995). The dataset represents the resultant directions of 22 sea stars 11 days after being displaced from their natural habitat, and the data are as below:

0, 1, 3, 3, 8, 13, 16, 18, 30, 31, 43, 45, 147, 298, 329, 332, 335, 340, 350, 354, 356, 357.

Figure 9 represents the graph of directions of 22 sea stars 11 days after being displaced from their natural habitat fitted to the proposed distribution.

Fifth dataset: The fifth dataset is taken from Fisher (1995) which presents the time series of 72 wind directions, comprising hourly measurements for three days at a site on

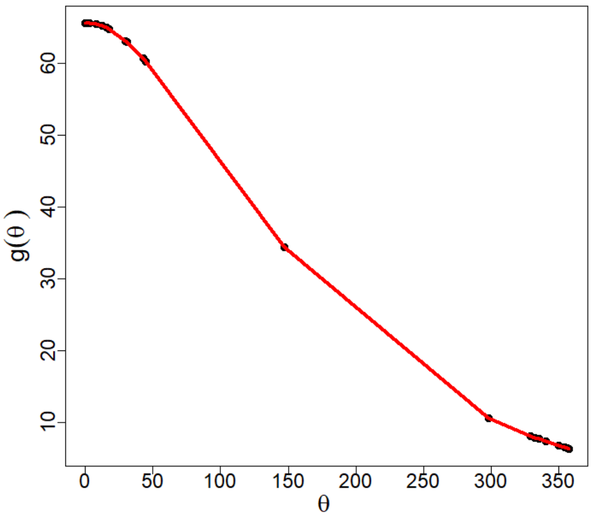

Figure 9: Graph of directions of 22 sea stars

Black Mountain, ACT, Australia. The data is provided below:

285, 285, 280, 300, 240, 255, 250, 250, 235, 240, 240, 180, 220, 265, 180, 150, 150, 150, 335, 355, 335, 305, 345, 340, 315, 0, 330, 300, 330, 330, 50, 270, 270, 270, 245, 285, 280, 270, 15, 285, 310, 330, 300, 340, 280, 300, 270, 270, 255, 90, 285, 285, 285, 270, 270, 270, 270, 270, 300, 300, 270, 300, 330, 15, 330, 300, 345, 330, 330, 300, 315, 285.

Table 6: Summary of statistics for WL, WTPL, WE, and WGL distributions for fourth dataset

Distribution	MLE	Log-likelihood	AIC	BIC	AICC
WL	$\lambda = 0.2592$	4.44	12.88	15.151	13.48
WTPL	$\theta = 0.0000371$ $\alpha = 0.0002602$	-1.691	0.617	2.973	1.189
WE	$\lambda = 1.81$	-0.465	3.069	5.34	3.669
WGL	$\lambda = 0.0865$ $\alpha = 0.0299$	-2.701	-1.401	0.955	-0.830

Figure 10 represents the graph of the fifth dataset fitted to the proposed distribution.

Firstly, it may be noted that all the five datasets taken into consideration are circular in nature which makes it appropriate for the proposed distribution to model these datasets. Secondly, all the distributions taken for comparison, are circular distributions that may be a particular case of Lindley distribution. It is to mention that the smaller values of Log-likelihood, AIC, BIC, and AICC indicate a better fit of distributions. As demonstrated in Table 3, Table 4, Table 5, Table 6, and Table 7, the Log-likelihood, AIC, BIC, and AICC have the lowest values for the WGL distribution. Hence, it can be said that the proposed

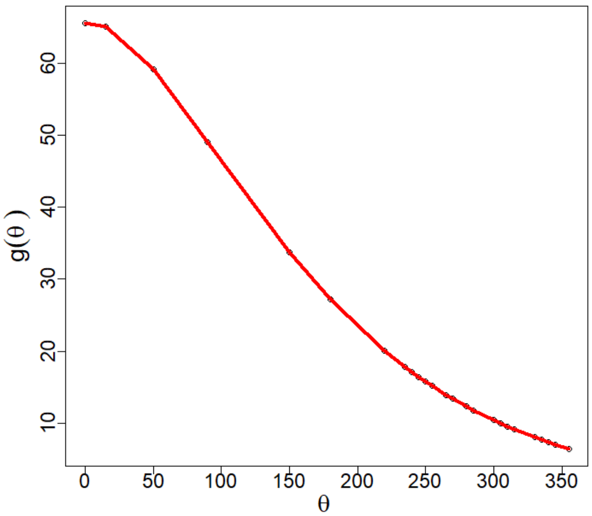

Figure 10: Graph of the time series of 72 wind directions

Table 7: Summary of statistics for WL, WTPL, WE, and WGL distributions for the fifth dataset

Distribution	MLE	Log-likelihood	AIC	BIC	AICC
WL	$\lambda = 0.0975$	-15.136	-26.271	-26.1	-21.691
WTPL	$\theta = 4.94 \times 10^{-02}$ $\alpha = 2.97 \times 10^{-11}$	-13.326	-22.651	-22.482	-18.043
WE	$\lambda = 5.16$	-36.192	-68.383	-68.212	-63.803
WGL	$\lambda = 0.0133$ $\alpha = 0.0268$	-39.869	-75.738	-71.130	-75.569

distribution fits well for all the datasets in comparison to other considered distributions.

9. Conclusion

To summarize, we have considered a new circular distribution by wrapping the generalized Lindley distribution, called the WGL distribution. The density and the distribution function of the proposed distribution were derived and expressions for characteristic functions, trigonometric moments, and other parameters have been discussed. The method of maximum likelihood estimation was used to estimate the model parameters. Further, a simulation study was conducted to show the consistency of the MLE. To show the applicability of the proposed distribution, we fit the WGL distribution to five circular datasets and compare the results with that of WL, WTPL, and WE distributions using Log-likelihood, AIC, BIC, and AICC test-statistics. Based on the above findings, it can be concluded that the WGL distribution provides the best fit for the given datasets than the other distributions taken into consideration.

Acknowledgements

The authors are indeed grateful to the Editors for their guidance and counsel. We would like to acknowledge the reviewers for their profound efforts in reviewing the manuscript and their valuable comments and suggestions, which immensely helped to improve the paper.

Conflict of interest

The authors do not have any financial or non-financial conflict of interest to declare for the research work included in this article.

References

Adnan, M. and Roy, S. (2014). Wrapped variance gamma distribution with an application to wind direction. *Journal of Environmental Statistics*, **6**, 1–10.

Coelho, C. A. (2007). The wrapped gamma distribution and wrapped sums and linear combinations of independent gamma and laplace distributions. *Journal of Statistical Theory and Practice*, **1**, 1–29.

Fisher, N. I. (1995). *Statistical Analysis of Circular Data.* cambridge university press.

Gatto, R. and Jammalamadaka, S. R. (2003). Inference for wrapped symmetric α-stable circular models. *Sankhyā: The Indian Journal of Statistics*, **65**, 333–355.

Jacob, S. and Jayakumar, K. (2013). Wrapped geometric distribution: A new probability model for circular data. *Journal of Statistical Theory and Applications*, **12**, 348–355.

Jammalamadaka, S. R., Bhadra, N., Chaturvedi, D., Kutty, T., Majumdar, P., and Poduval, G. (1986). Functional assessment of knee and ankle during level walking. *Data Analysis in Life Science*, 21–54.

Jammalamadaka, S. R. and Kozubowski, T. J. (2004). New families of wrapped distributions for modeling skew circular data. *Communications in Statistics-Theory and Methods*, **33**, 2059–2074.

Jammalamadaka, S. R. and Sengupta, A. (2001). *Topics in Circular Statistics*, volume 5. world scientific.

Joshi, S. and Jose, K. (2018). Wrapped lindley distribution. *Communications in Statistics-Theory and Methods*, **47**, 1013–1021.

Lindley, D. V. (1958). Fiducial distributions and Bayes' theorem. *Journal of the Royal Statistical Society. Series B (Methodological)*, **20** 102–107.

Mardia, K. V. and Jupp, P. E. (2000). *Directional Statistics.* John Wiley & Sons.

Pewsey, A. (2008). The wrapped stable family of distributions as a flexible model for circular data. *Computational Statistics & Data Analysis*, **52**, 1516–1523.

Pewsey, A., Lewis, T., and Jones, M. (2007). The wrapped t family of circular distributions. *Australian & New Zealand Journal of Statistics*, **49**, 79–91.

PL, L. (1939). Addition of random variables defined on a circumference. *Bulletin of the Mathematical Society of France*, **67**, 1–41.

Rao, J. S. and Sengupta, S. (1972). Mathematical techniques for paleocurrent analysis: Treatment of directional data. *Journal of the International Association for Mathematical Geology*, **4**, 235–248.

Roy, S. and Adnan, M. (2012). Wrapped generalized gompertz distribution: An application to ornithology. *Journal of Biometrics & Biostatistics*, **3**, 1–4.

Sarma, R., Dattatreya Rao, A., and Girija, S. (2011). On characteristic functions of the wrapped lognormal and the wrapped weibull distributions. *Journal of Statistical Computation and Simulation*, **81**, 579–589.

Shanker, R., Sharma, S., Shanker, U., and Shanker, R. (2013). Janardan distribution and its application to waiting times data. *Indian Journal of Applied Research*, **3**, 500–502.

Upton, G. J. (1985). *Spatial Data Analysis by Example: Categorical and Directional Data*, volume 2. Wiley.